Microwave Assisted Combustion Synthesis of Co-Zn Nanoparticles Ferrite Encapsulation by Graphene

Nada S. Ahmade and Falah M. Abdel Hasan
Department of Physics, College of Science, University of Diyala, Diyala, Iraq

Abstract: In this research, we have used a microwave assisted combustion method to synthesize cobalt-zinc ferrite nanoparticles with four nanocrystalline ferrites including : $Co_1Fe_2O_4$, $Co_{0.9}Zn_{0.1}Fe_2O_4$, $Co_{1.1}Zn_{0.1}Fe_2O_4$ and $Co_{0.3}Zn_{0.7}Fe_2O_4$ using glycine as a fuel. Then syntheses graphene by the same method, graphene single layer graphite, known as graphene is an important material because of its unique two-dimensional structure, high conductivity, excellent electron mobility and high surface area. The obtained ferrites were characterized studied by X-Ray powder Diffraction (XRD), results for Co-Zn ferrite after and before coating via. graphene showed that the material had cubic spinal structure. Field Emission Scanning Electron Microscopy (FESEM) micrographs for the powder before coating showed that all of the nanoparticles have nano-crystalline behavior (16-36 nm) and particles indication cubic shape and after coating via grapheme was (46-12 nm). Vabrating VSM analysis demonstrated that the type of fuel used for synthesis is highly effective a parameter on magnetic properties of nanoparticles. The B-H loops of all samples that are obtained by using vibrating sample magnetometer are displayed. The effect of Co addition on saturation magnetization and the coercivity of all the samples are discussed. The samples synthesized with glycine fuel showed better magnetic properties for application as soft magnetic devices.

Key words: High conductivity, Co-Zn ferrite, nanoparticles, vabrating VSM, demonstrated, glycine fuel

INTRODUCTION

Magnetic nanoparticles are substance to intense research because they possess attractive properties which could see potential use in catalysis, biomedicine and environmental remediation (Liu and Zhang, 2010). Between the magnetic nanoparticles, nanosized cobalt zinc ferrite (Co-$ZnFe_2O_4$) particles are occupying an important place for their unusual properties for example magnetocrystalline anisotropy, high coercivity and moderate saturation magnetization (Wakeland *et al.*, 2010).

Graphene is the eventually monolayer material of carbon with single-atom thickness. It possesses many fascinating properties including high mobility, unusual high thermal conductivity, stiffness and strength. Impressively these properties have remarkable dependence on its morphology and atomic structure, e.g., its size and shape. Also, interior and exterior doping effects from defects, molecular adsorptions or electromagnetic fields are too significant. For example, hydrogenation, oxidation and electrical field significantly tune its structural, mechanical, thermal, electronic and optical properties which is controllable and even reversible. These reactions of a graphene sheets to structural and environmental effects attract the scientists to engineer its physical and chemical properties at nanoscale (Soldano *et al.*, 2010).

Microwaves are electromagnetic waves with wavelengths from 1 mm^{-1} m and corresponding frequencies between 300 MHz and 300, 0.915 and 2.45 GHz frequencies are usually, used for microwave heating (Shin *et al.*, 2012). These frequencies are chosen for the microwave heating based in two reasons. The first is that they are in one of the Industrial, Scientific and Medical (ISM) radio bands set aside for non-communication purposes. The second is that the penetration complexity of the microwaves is greater for these low frequencies (Hischier and Walser, 2012). Generally, materials can be classified into three categories based on their interaction with microwaves: materials that reflect microwaves, characterized by bulk metals and alloys, e.g., copper; materials that are transparent to microwaves.

Magnetic Nanoparticles (MNPs), except the selection of a suitable magnetic core, fine tuning of surface coating materials represents a major challenge for the practical usage of MNPs in clinical applications (Giordano and Antonietti, 2011). The coating can consist of long-chain organic ligans or inorganic/organic polymers where these ligands or polymers container be introduced during

---

Corresponding Author: Nada S. Ahmade, Department of Physics, College of Science, University of Diyala, Diyala, Iraq

(*in-situ* coating) or after (post-synthetic coating) synthesis. During the *in-situ* coating which is the procedure followed in co-precipitation synthesis technique, precursors of magnetic cores and coating materials are dissolved in the similar reaction solution and the nucleation of magnetic core and the coating occurs simultaneously. On the contrary in post-synthetic coating which is the case in MNP synthesis with thermal decomposition technique, the surface coating materials are presented after the formation of magnetic cores. In both procedures in order to link the surface molecules to magnetic cores, generally two different approaches; either end-grafting or surface-encapsulation are followed. In the former one, the coating molecules are anchored on magnetic core by the help of a single capping group at their one end whereas in the latter usually polymers, already carrying multiple active groups are attached on the surface of magnetic core with manifold connections resulting stronger and more stable coatings (Valizadeh *et al.*, 2012).

MATERIALS AND METHODS

Experimental work
Preparation of graphene: The glycine is dissolved in distilled water in a glass beaker over the magnetic hot plat-stirrers model SH-2 for 10 min then the graphite powder is added to the mixture and the mixture stays on the hot plat-stirrers for half an hour. The mixture is poured into a glass flask of quartz and the hole is sealed with aluminum foil to prevent its volatilization. And put in microwave oven (1200 W) For 20 min then the graphene powder is obtained.

Surface coating by graphene: Cobalt nitrate, zinc nitrate, ferric nitrate were mixed in certain stoichiometric ratios with appropriate amount of distilled water in glass beaker and mixed well at room temperature by magnetic hot plat-stirrers model SH-2 with high velocities. Then, add glycine used as foul in the preparation and mixed well at room temperature by magnetic hot plat-stirrers for 10 min, so, the solution become black color. Then add graphene powder on the mixture and stay in the magnetic hot plat-stirrers for 30 min. The mixture is then placed in glass tubes that are closed and packed in the ultra-sonic for 40 min at 70°C. Then pour into a quartz glass flask and sit in the microwave oven for 20 min to obtain the ferrite coating via. graphene.

RESULTS AND DISCUSSION

XRD analysis were performed for the structural characterization of the synthesized nanoparticles. X-Ray

Table 1: Structural parameters of co-zn ferrite by glycine

Formula	2θ	d (A)	α (A)	D (nm)
$Co_1Fe_2O_4$	33.52	2.5248	8.3738	28.18
$Co_{0.9}Zn_{0.1}Fe_2O_4$	30.36	2.1316	7.0699	28.08
$Co_{1.1}Zn_{0.1}Fe_2O_4$	33.90	1.6167	5.3619	37.20
$Co_{0.3}Zn_{0.7}Fe_2O_4$	34.69	1.6223	5.3806	29.42

Diffraction (XRD) analysis were performed with Cu Kα irradiation (λ = 1.5418 Å) in the 2θ range 10-80°. The crystallite size of the $CoFe_2O_4$ NPs was based on X-ray diffraction line broadening and calculated by using Scherrer's Eq. 8:

$$D = B\lambda/\beta\cos\phi \qquad (1)$$

Where:
D = The average crystallite size of the phase under investigation
B = The Scherrer's constant (0.89)
λ = The wave length of X-ray beam used
β = The full-width half maximum of diffraction peak
θ = The Bragg's angle

The lattice parameter "a" was calculated according to the Eq. 8 (Table 1):

$$a = d_{hkl}(h^2+k^2+l^2)1/2 \qquad (2)$$

X-ray analysis performs to identify the atomic and molecular structure of a crystal. XRD is one of the main analyses in the determining of the structure. The synthesis mixture prepared in stoichiometric rates was put in to the kitchen type microwave oven. Agreeing the XRD patterns given in Fig. 1, narrow and sharp reflection peaks were observed in the measured diffraction pattern for two fuel types. Moreover, it can be supposed that the glycine have the most significant positive effect on the crystal structure and the conversion (Wu *et al.*, 2012). The diffraction patterns of $CoZnFe_2O_4$ consisted of peaks corresponding to crystallographic planes 220, 311, 400, 422, 511 and 440. All the observed peaks and Miller indices (hkl) of the fcc lattice were in agreement with the reported values (Chang *et al.*, 2012; Bykkam *et al.*, 2013). The crystallite size of the samples prepared by different approaches was in the range of 16-35 nm, respectively. The difference in crystallite size was due to different preparation conditions for ferrite synthesis. The lattice parameter of as prepared samples, according to the cubic crystal structure calculated from the main peak of spinel structure (311) using Eq. 2. Scherrer's equationused to calculated the crystallite size (D) from Eq. 1. The substituted zinc ions in cobalt ferrite led to large increase in lattice constant after this value the lattice parameter have small increase in values. While crystallite size decrease with zinc ions this refer to the zinc ions replaced
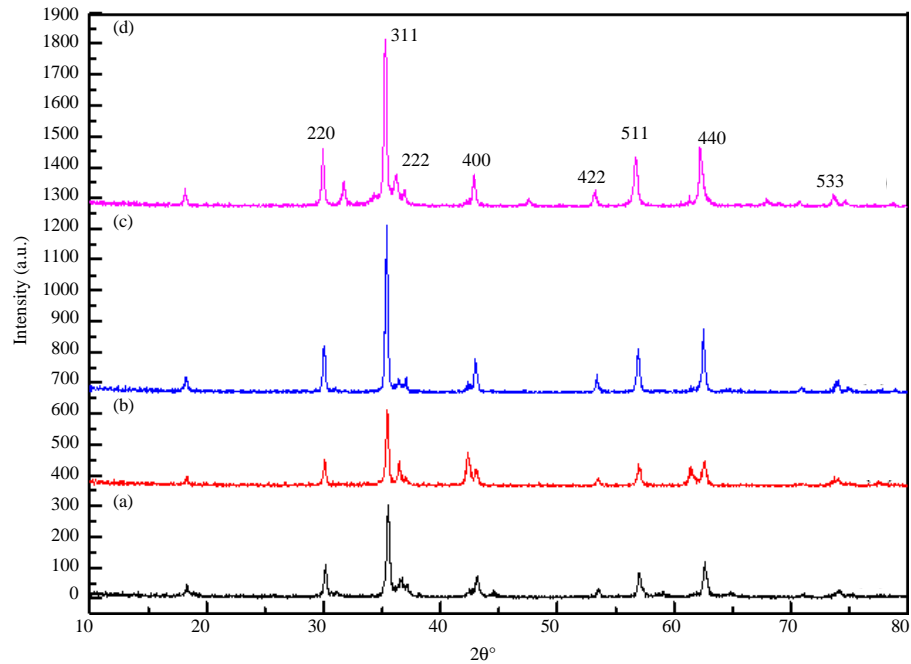
Fig. 1: XRD patterns of the samples obtained by glycine: a) $Co_1Fe_2O_4$; b) $Co_{0.9}Zn_{0.1}Fe_2O_4$; c) $Co_{1.1}Zn_{0.1}Fe_2O_4$ and d) $Co_{0.3}Zn_{0.7}Fe_2O_4$
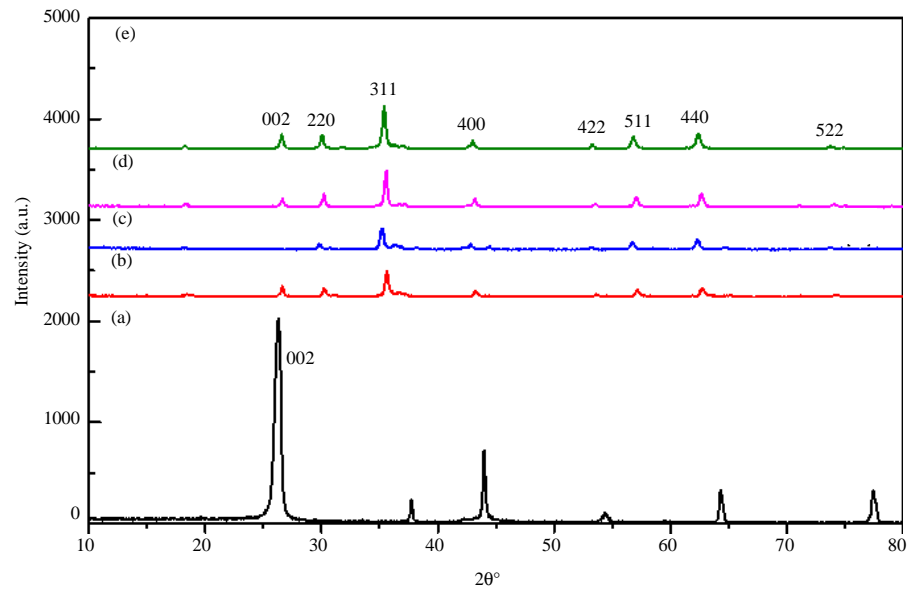

Fig. 2: XRD patterns of the samples obtained by glycine: a) Graphen pure; b) $Co_1Fe_2O_4$ with graphene; c) $Co_{0.9}Zn_{0.1}Fe_2O_4$ with graphene; d) $Co_{1.1}Zn_{0.1}Fe_2O_4$ with graphene and e) $Co_{0.3}Zn_{0.7}Fe_2O_4$ with graphene

with cobalt ionswhich may be attributed to the smaller ionic radii of Zn^{2+} ions (0.6Å) as compared to co^{2+} (0.79 Å) cations (Jana *et al.*, 2017).

XRD analysis were coating co-zn ferrite via. graphene: The diffraction peaks could be assigned from Fig. 2 which correspond to 002, 220, 311, 222, 400, 422, 511 and 440 planes of Co-Zn ferrite, respectively. As shows in Fig. 2, the peaks were in moral agreement with value of repretes (Cristea *et al.*, 2017) which indicate the samples had a face-centered cubic crystal structure. No secondary impurity phase was detected, hence, the

absence of additional peaks assigned in the sample (c) to the graphene plane. This fundsgraphene with ferrite nano-particles are relatively coated. The broadening of the diffraction peaks indicates the nano-crystalline nature of the materials. As shows in Fig. 2, the XRD peaks planes (002) were caused by the paraffin because of its regular crystallization (Fu *et al.*, 2012). The calculated mean crystallite size value of Co-Zn ferrite is found to be about 33 nm. The lattice constant (aexp) was calculated and found to be 5.3 (Table 2).

Magnetic properties: The magnetization of the present samples was obtained using VSM at RT with an applied field $\pm 10 \, kO_e$. The observed hysteresis loops from VSM

are shows in Fig. 3a-h. The magnetic properties of the prepared samples are analyzed using a magnetometer (VSM) at room temperature. Figure 3 shows the M-H curves of the prepared samples. The loop is narrow which means the papered samples are soft magnetic material. The saturation Magnetization (M_s) and coercivity (H_c) values have been directly extracted from these curves as in insert of Figures and have been listed in various Co

Table 2: Structural parameters of co-zn ferrite coating via. graphene

Formula	2θ	d (A)	α (A)	D (nm)
$Co_1Fe_2O_4$	36.93	2.4316	8.51038	22.52
$Co_{0.9}Zn_{0.1}Fe_2O_4$	35.72	2.5113	7.03990	42.23
$Co_{1.1}Zn_{0.1}Fe_2O_4$	36.49	2.4599	5.32290	33.42
$Co_{0.3}Zn_{0.7}Fe_2O_4$	35.77	2.5077	5.40060	35.72
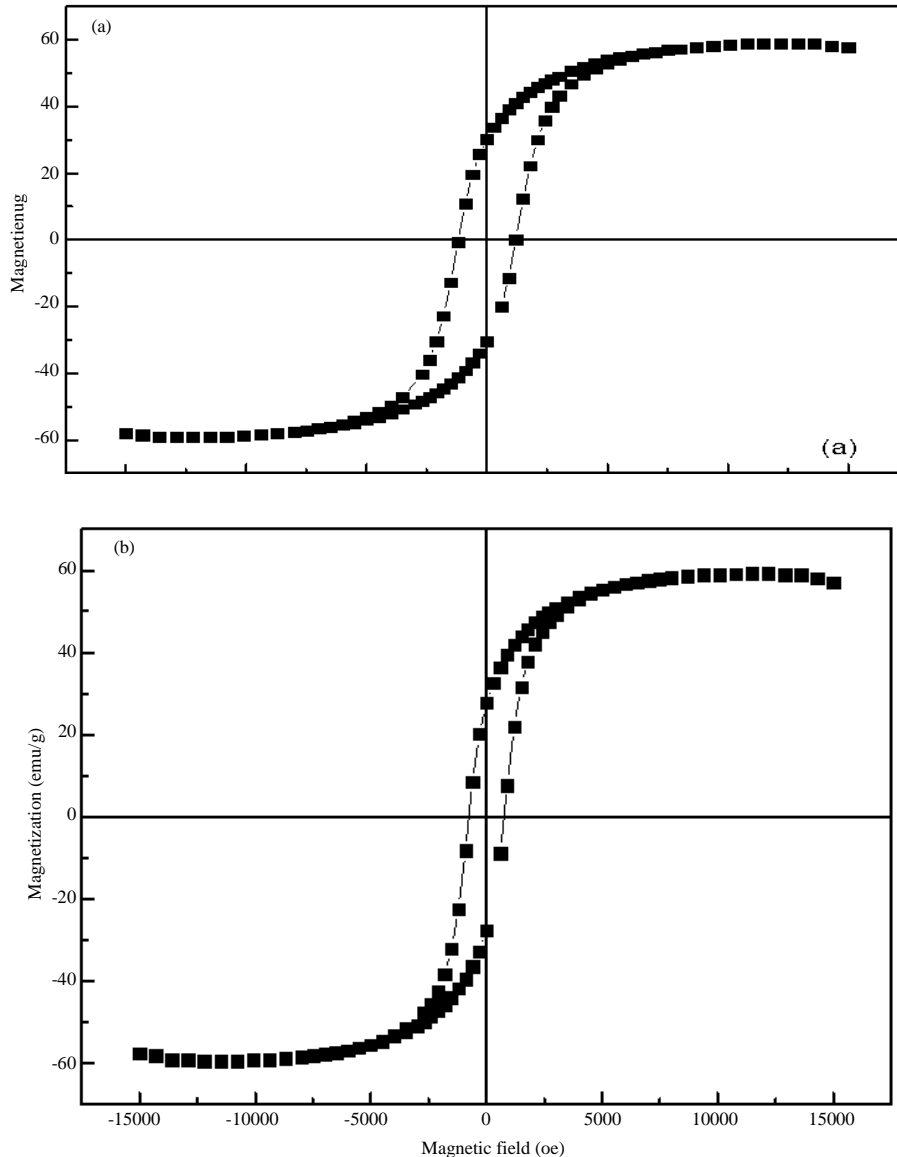
Fig. 3: Continue
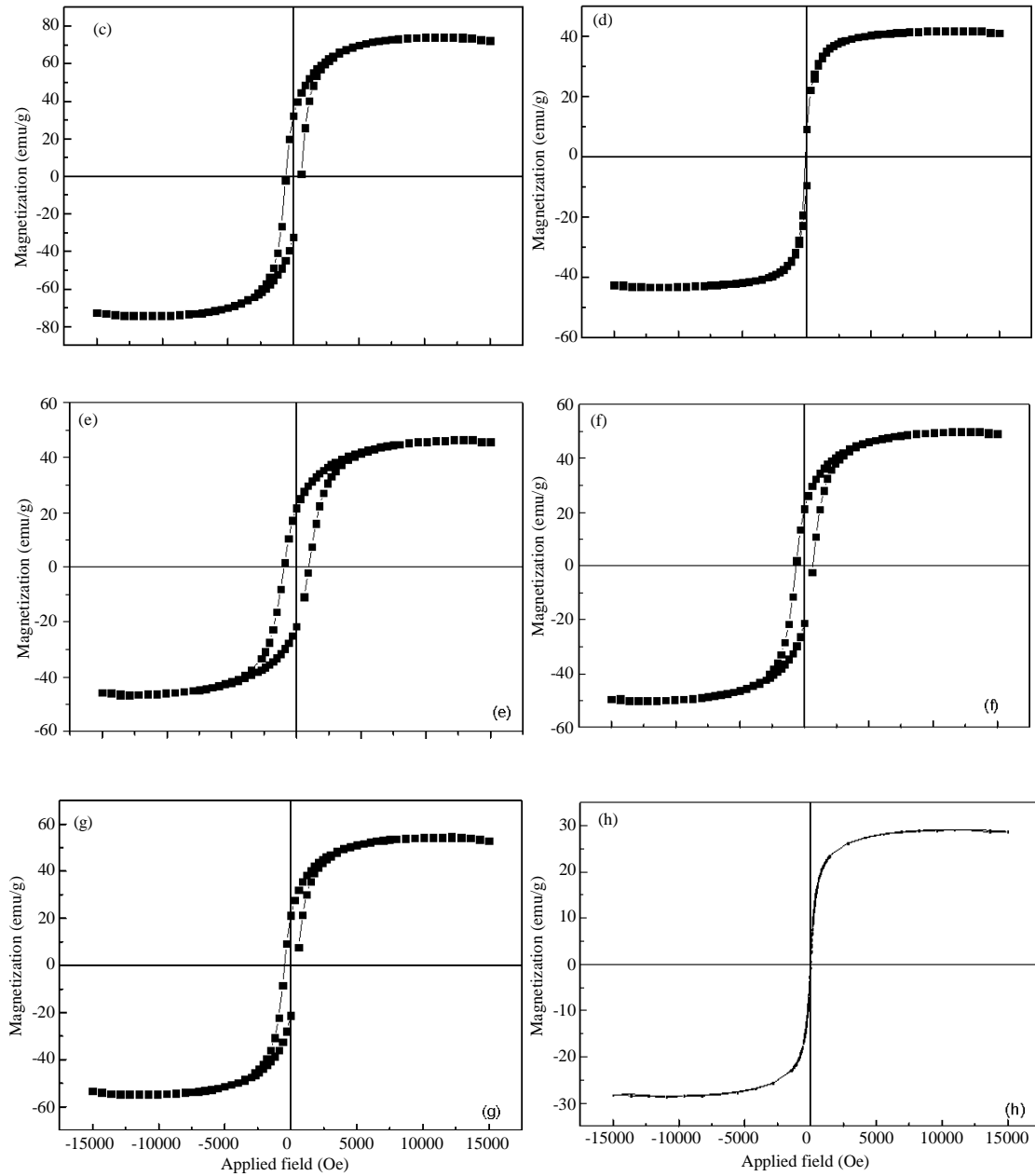
Fig. 3: Magnetic hysteresis loops; a) $Co_1Fe_2O_4$ by glycine as foul; b) $Co_{0.9}Zn_{0.1}Fe_2O_4$ by glycine as foul; c) $Co_{1.1}Zn_{0.1}Fe_2O_4$ by glycine as foul; d) $Co_{0.3}Zn_{0.7}Fe_2O_4$ by glycine as foul; e) $Co_1Fe_2O_4$ with graphene; f) $Co_{0.9}Zn_{0.1}Fe_2O_4$ with graphene; g) $Co_{1.1}Zn_{0.1}Fe_2O_4$ with graphene and h) $Co_{0.3}Zn_{0.7}Fe_2O_4$ with graphene

content in Table 3. the saturation magnetization and coercivity increase with Co content. The behavior of the saturation magnetization can be explained because of cations distribution and super-exchange interactions. The saturation magnetization increase as crystallite size increases with a maximum value of $M_s = 74.245$ emu/g (D = 37.20 nm) for glycine and then decrease with further

Table 3: Magnetic properties of cobalt zinc ferrite by glycine as foul

Formula	M_s (emu/g)	H_c (Oe)	M_r (emu/g)	$S = M_r/M_s$
$Co_1Fe_2O_4$	58.7020	1200	30.337	0.525
$Co_{0.9}Zn_{0.1}Fe_2O_4$	59.157	900	27.63	0.483
$Co_{1.1}Zn_{0.1}Fe_2O_4$	74.245	600	32.2933	0.447
$Co_{0.3}Zn_{0.7}Fe_2O_4$	45.136	300	9.297	0.226

increase in crystallite size. The coercivity change with (D). On the other hand, to explain the impact of reducing

domain, squareness ratio M_r/M_s computed for each sample, 0.2-0.4, 0.5 for glycine. Values of squareness ratio vary between 0.2 and 0.5. When the ratio between remanence and saturation magnetization <(0.5) the materials have single domain but if the ratio larger than (0.5) the materials possess multi domain synthesis (Bai *et al.*, 2012), M_r/M_s ratio exhibited below the range that is meant the samples have single domain structures (Reddy and Yun, 2016).

Figure 4a-h shows the M-H curves of the prepared samples. The loop is more narrow than Fig. 3 which means the papered samples are soft magnetic material closed to super para magnetic. The saturation Magnetization (M_s) and Coercivity (H_C) values have been directly extracted from these curves as in insert of Figures and have been listed in various Co content in Table 4. The saturation magnetization and coercivity increase with Co content. The behavior of the saturation magnetization can be explained because of cations distribution and super-exchange interactions. The saturation magnetization increase as crystallite size increases with a maximum value of M_s = 80.265 emu/g (D = 33.42 nm) for

glycine coating with graphene and then decrease with further increase in crystallite size. The coercivity change with (D). On the other hand, toexplain the impact of reducing domain, squareness ratio M_r/M_s computed for each sample, 0.3-0.4, 0.5 for glycine. Values of squareness ratio vary between 0.3 and 0.5. When the ratio between remanence and saturation magnetization <(0.5) the materials have single domain but if the ratio larger than (0.5) the materials possess multi domain synthesis (Bykkam *et al.*, 2013; Jana *et al.*, 2017), M_r/M_s ratio exhibited below the range that is meant the samples have single domain structures (Fu *et al.*, 2012).

Morphology measurements: To show the morphology of sample the FESEM images have been taken in Fig. 5 and 6. Note that the average grain size of the sample obtained from FESEM images is larger than nanocrystals size which determined by the XRD measurement which simply indicates to the agglomeration in the nanoparticles. The samples are spherical, uniform and having a distribution size (16-36 nm) before and (12-46) after coating by graphene.
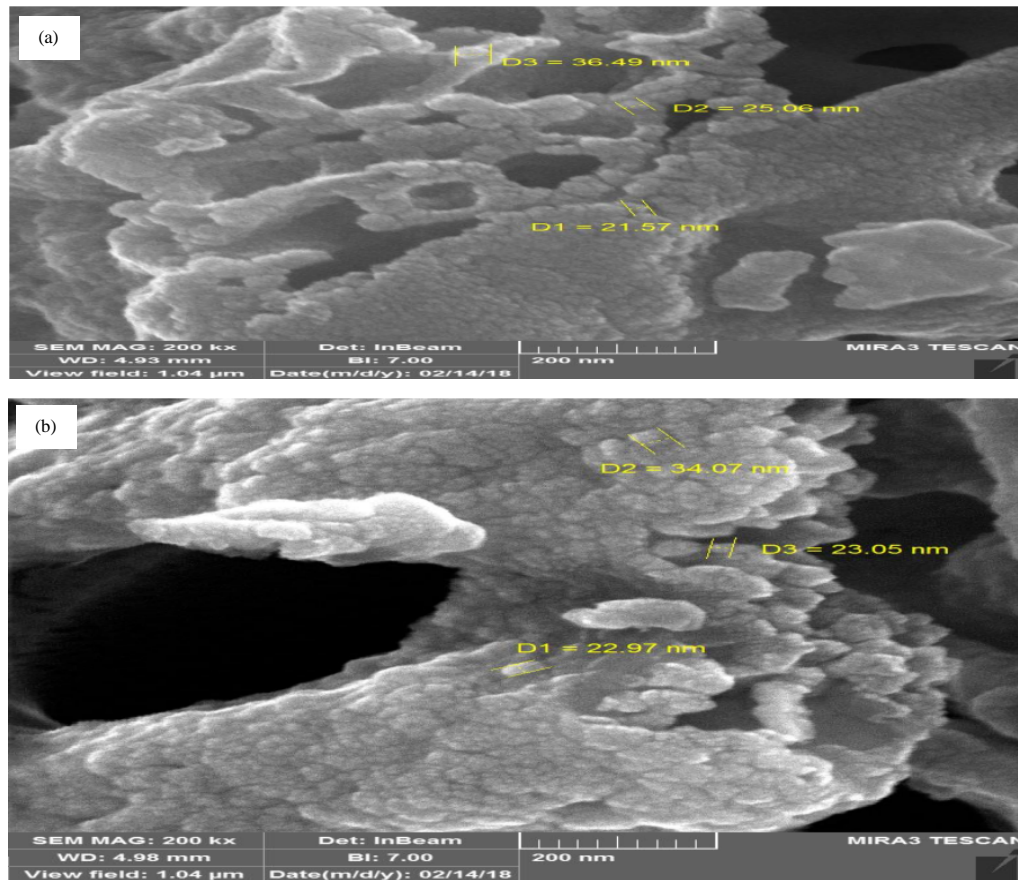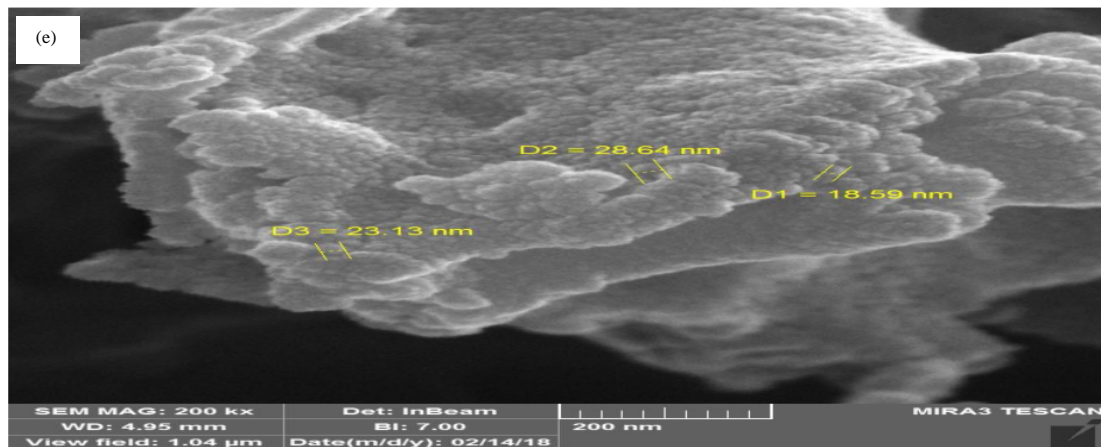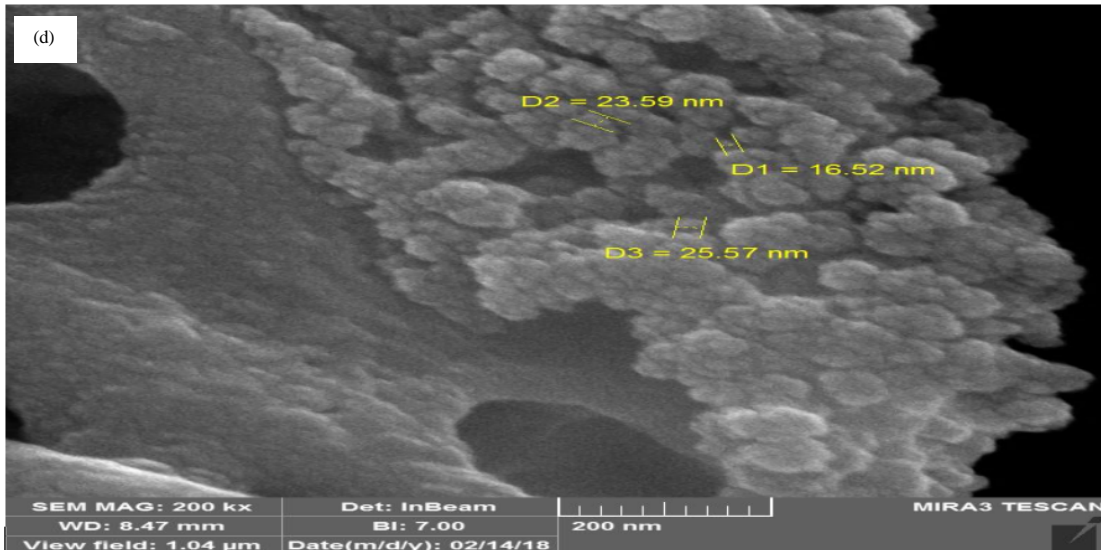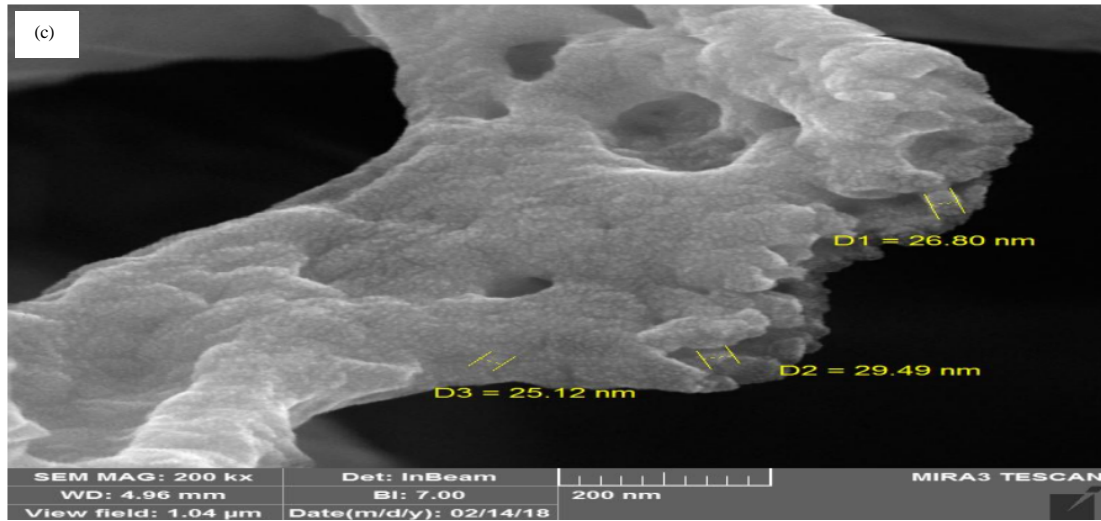

Fig. 4: Continue

Fig. 4: Continue
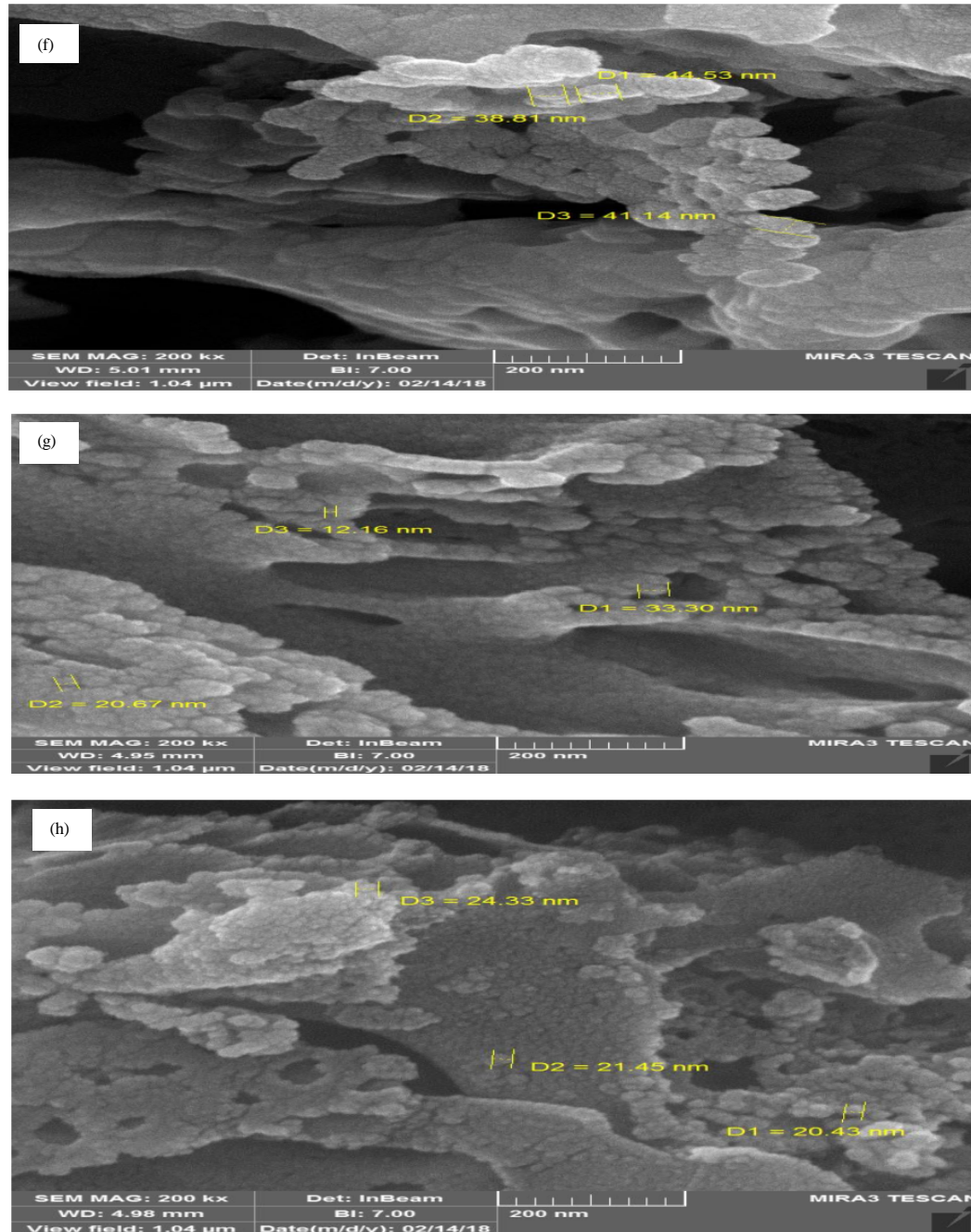
Fig. 4: FESEM image of the samples obtained by glycine: a) $Co_1Fe_2O_4$; b) $Co_{0.9}Zn_{0.1}Fe_2O_4$; c) $Co_{1.1}Zn_{0.1}Fe_2O_4$; d) $Co_{0.3}Zn_{0.7}Fe_2O_4$; e) $Co_1Fe_2O_4$ with graphene; f) $Co_{0.9}Zn_{0.1}Fe_2O_4$ with graphene; g) $Co_{1.1}Zn_{0.1}Fe_2O_4$ with graphene and h) $Co_{0.3}Zn_{0.7}Fe_2O_4$ with graphene

CONCLUSION

Ferrites have been studied and applied for more than 50 years and are considered as well-known materials with "mature" technologies to microwave devices. However, the advances in applications and fabrication technologies in the last 10 years have been impressive. Microwave assisted combustion method with an important method in quick, simple and low cost at synthesis of the nanoparticles. Bulk ferrites remain a key group of

magnetic materials while nanostructured ferrites show affected promise for applications in even significantly wider fields. Combustion reaction synthesis using glycine as fuel managed the formation of monophasic crystalline. The average crystallite size of the powders synthesized with glycine was rang 16-36 nm. The use of graphene as a refractory coating has improved the properties of the surface in terms of reducing toxicity and solubility in the case of its use in the medical application as well as of its magnetic propertiesby the (VSM) and is preparation by a microwave method.

REFERENCES

Bai, S., X. Shen, X. Zhong, Y. Liu and Z. Zhu, 2012. One-pot solvothermal preparation of magnetic reduced graphene oxide-ferrite hybrids for organic dye removal. Carbon, 50: 2337-2346.

Bykkam, S., K.V. Rao, C.H.S. Chakra and T. Thunugunta, 2013. Synthesis and characterization of graphene oxide and its antimicrobial activity against klebseilla and staphylococus. Intl. J. Adv. Biotechnol. Res., 4: 142-146.

Chang, B.Y.S., N.M. Huang, M.A. An'amt, A.R. Marlinda and Y. Norazriena *et al.*, 2012. Facile hydrothermal preparation of titanium dioxide decorated reduced graphene oxide nanocomposite. Intl. J. Nanomed., 7: 3379-3387.

Cristea, C., M. Tertis and R. Galatus, 2017. Magnetic nanoparticles for antibiotics detection. Nanomater., 7: 119-119.

Fu, Y., H. Chen, X. Sun and X. Wang, 2012. Combination of cobalt ferrite and graphene: High-performance and recyclable visible-light photocatalysis. Appl. Catal. B. Environ., 111: 280-287.

Giordano, C. and M. Antonietti, 2011. Synthesis of crystalline metal nitride and metal carbide nanostructures by sol-gel chemistry. Nano Today, 6: 366-380.

Hischier, R. and T. Walser, 2012. Life cycle assessment of engineered nanomaterials: State of the art and strategies to overcome existing gaps. Sci. Total Environ., 425: 271-282.

Jana, A., E. Scheer and S. Polarz, 2017. Synthesis of graphene-transition metal oxide hybrid nanoparticles and their application in various fields. Beilstein J. Nanotechnol., 8: 688-714.

Liu, F. and Y. Zhang, 2010. Substrate-free synthesis of large area, continuous multi-layer graphene film. Carbon, 48: 2394-2400.

Reddy, D.H.K. and Y.S. Yun, 2016. Spinel ferrite magnetic adsorbents: Alternative future materials for water purification?. Coord. Chem. Rev., 315: 90-111.

Shin, D., S. Bae, C. Yan, B.H. Hong and J. Ryu *et al.*, 2012. Synthesis and applications of graphene electrodes. Carbon Lett., 13: 1-16.

Soldano, C., A. Mahmood and E. Dujardin, 2010. Production, properties and potential of graphene. Carbon, 48: 2127-2150.

Valizadeh, A., H. Mikaeili, M. Samiei, S.M. Farkhani and N. Zarghami *et al.*, 2012. Quantum dots: Synthesis, bioapplications and toxicity. Nanoscale Res. Lett., 7: 1-14.

Wakeland, S., R. Martinez, J.K. Grey and C.C. Luhrs, 2010. Production of graphene from graphite oxide using urea as expansion-reduction agent. Carbon, 48: 3463-3470.

Wu, M.S., Y.P. Lin, C.H. Lin and J.T. Lee, 2012. Formation of nano-scaled crevices and spacers in NiO-attached graphene oxide nanosheets for supercapacitors. J. Mater. Chem., 22: 2442-2448.